SYNTHESIS OF RARE EARTH COMPOUNDS AND STUDY OF THEIR MAGNETIC OPTICAL AND SEMICONDUCTING PROPERTIES

IBM Corporation
Thomas J. Watson Research Center
Yorktown Heights, New York 10598

SEMIANNUAL TECHNICAL REPORT

30 June 1971 to 31 December 1971

Contract No. DAAH01-71-C-1313

38

Sponsored by

Advanced Research Project Agency
ARPA Order No. 1588

ARPA Support Office - Army Missile Command
Directorate for Research, Development,
Engineering and Missile Systems Laboratory
U. S. Army Missile Command
Redstone Arsenal, Alabama

SYNTHESIS OF RARE EARTH COMPOUNDS AND STUDY OF THEIR MAGNETIC OPTICAL AND SEMICONDUCTING PROPERTIES

IBM Corporation
Thomas J. Watson Research Center
Yorktown Heights, New York 10598

SEMIANNUAL TECHNICAL REPORT

30 June 1971 to 31 December 1971

Contract No. DAAH01-71-C-1313

Sponsored by

Advanced Research Project Agency
ARPA Order No. 1588

ARPA Support Office - Army Missile Command
Directorate for Research, Development,
Engineering and Missile Systems Laboratory
U. S. Army Missile Command
Redstone Arsenal, Alabama

NOTICE

"This research was sponsored by the Advanced Research Projects Agency of the Department of Defense under ARPA Order No. 1588 and was monitored by the U. S. Army Missile Command under Contract No. DAAH01-71-C-1313. Views and conclusions expressed herein are the primary responsibility of the author or the contractor and should not be interpreted as representing the official opinion or policy of USAMICOM, ARPA, DOD or any other agency of the Government."

FOREWORD

This report describes work performed under Contract DAAH01-71-C01313 for the ARPA Support Office, Research, Development, Engineering and Missiles Laboratory, U. S. Army Missile Command, Redstone Arsenal, Alabama during the period 30 June 1971 through 31 December 1971. The monitors for this project were R. L. Norman and S. L. Johnston. The principal investigator was F. Holtzberg and the report was written by F. Holtzberg, T. R. McGuire, T. Penney, M. W. Shafer and S. von Molnar. The work was performed at the IBM Thomas J. Watson Research Center. The authors gratefully acknowledge the technical assistance of R. B. Hamilton, R. A. Figat, H. R. Lilienthal, P. G. Lockwood and J. M. Rigotty, and the support of R. W. Johnson, B. L. Olson, J. D. Kuptsis and W. Reuter who provided the following analytical techniques: Solid state mass spectroscopy, classical chemical analysis and quantitative electron probe microanalysis.

Unclassified

Security Classification

DOCUMENT CONTROL DATA - R & D

(Security classification of title, body of abstract and indexing annotation must be entered when the overall report is classified)

1. ORIGINATING ACTIVITY (Corporate author)
International Business Machines Corporation
Thomas J. Watson Research Center, P. O. Box 218
Yorktown Heights, New York 10598

2a. REPORT SECURITY CLASSIFICATION
Unclassified

2b. GROUP

3. REPORT TITLE
RESEARCH IN THE SYNTHESIS OF RARE EARTH COMPOUNDS AND A STUDY OF THEIR MAGNETIC OPTICAL AND SEMICONDUCTING PROPERTIES

4. DESCRIPTIVE NOTES (Type of report and inclusive dates)
Semiannual Technical Report (30 June 1971 to 31 December 1971)

5. AUTHOR(S) (First name, middle initial, last name)
F. Holtzberg, T. R. McGuire, T. Penney, M. W. Shafer and S. von Molnar

6. REPORT DATE	7a. TOTAL NO. OF PAGES	7b. NO. OF REFS
January 1972	31	20

8a. CONTRACT OR GRANT NO.	9a. ORIGINATOR'S REPORT NUMBER(S)
DAAH01-71-C-1313	IBM Project # 2552
b. PROJECT NO.	
c.	9b. OTHER REPORT NO(S) (Any other numbers that may be assigned this report)
d.	

10. DISTRIBUTION STATEMENT
Distribution of this document is unlimited.

11. SUPPLEMENTARY NOTES	12. SPONSORING MILITARY ACTIVITY
	Advanced Research Project Agency Arlington, Virginia 22209 ARPA Order No. 1588

13. ABSTRACT

We have pursued the study of chemical equilibria involved in the synthesis and crystal growth of pure rare earth chalcogenides. We have continued to explore the relationship of defect structure and variations in stoichiometry to the physical properties of these materials. This report contains the results of investigations of three different systems which have in common magnetic rare earth ions and a range of homogeneity over which the change in defect structures leads to large changes in the interaction between magnetic ordering and transport.

In the europium oxygen system conductivity, infrared absorption, microstructure and growth parameters of EuO crystals of varying stoichiometry have been correlated and used to determine a new phase diagram.

The transport properties of single crystal ferromagnetic $Gd_{3-x}v_xS_4$, where v denotes denotes vacancies and x is near 1/3, have been interpreted in terms of the concept of localization of electron states first suggested for paramagnetic $Ce_{3-x}v_xS_4$ by Cutler and Mott and extended here to include magnetic interactions.

The range of homogeneity has been studied in the face centered cubic Gd_xSe_{1-x} system. The solid solution field is bounded by the composition x = 0.443 for excess Se and extends through the stoichiometric composition to at least 0.512 for excess Gd. The lattice constant decreases linearly with decreasing Gd concentration except at lowest values of x. The materials have been characterized by resistivity, reflectivity and magnetic measurements. The results of the transport and reflectivity measurements are explained on the basis of a simple single rigid band model. Magnetization measurements show that all compositions order antiferromagnetically with the Néel temperature, T_N, varying from $\sim 20°$ to $\sim 60°$K and θ from -25 to -135°K with increasing Gd or electron concentration.

DD FORM 1 NOV 65 1473

Security Classification

14. KEY WORDS	LINK A		LINK B		LINK C	
	ROLE	WT	ROLE	WT	ROLE	WT
Semiconducting ferromagnets						
Europium oxide						
Synthesis						
Nonstoichiometry						
Crystal growth						
Rare earths						
$Gd_{3-x}V_xS_4$						
GdSe						

SUMMARY

We have pursued the study of chemical equilibria involved in the synthesis and crystal growth of pure rare earth chalcogenides. We have continued to explore the relationship of defect structure and variations in stoichiometry to the physical properties of these materials. This report contains the results of investigations of three different systems which have in common magnetic rare earth ions and a range of homogeneity over which the change in defect structures leads to large changes in the interaction between magnetic ordering and transport.

In the europium oxygen system conductivity, infrared absorption, microstructure and growth parameters of EuO crystals of varying stoichiometry have been correlated and used to determine a new phase diagram.

The transport properties of single crystal ferromagnetic $Gd_{3-x}v_xS_4$, where v denotes vacancies and x is near 1/3, have been interpreted in terms of the concept of localization of electron states first suggested for paramagnetic $Ce_{3-x}v_xS_4$ by Cutler and Mott and extended here to include magnetic interactions.

The range of homogeneity has been studied in the face centered cubic Gd_xSe_{1-x} system. The solid solution field is bounded by the composition $x = 0.443$ for excess Se and extends through the stoichiometric composition to at least 0.512 for excess Gd. The lattice constant decreases linearly with decreasing Gd concentration except at lowest values of x. The materials have been characterized by resistivity, reflectivity and magnetic measurements. The results of the transpor and reflectivity measurements are explained on the basis of a simple single rigid band model. Magnetization measurements show

that all compositions order antiferromagnetically with the Néel temperature, T_N, varying from $\sim 20°$ to $\sim 60°K$ and θ from -25 to -135°K with increasing Gd or electron concentration.

TABLE OF CONTENTS

1.0 INTRODUCTION

In the previous contract (DAAH01-70-C-1309) we demonstrated that the europium monochalcogenides exist over a range of compositions. Although this homogeneity range is relatively narrow, the effective change in carrier concentration with compositional changes results in dramatic variations in magnetic, optical and transport properties of these systems.

We have explored the EuO system in detail and have correlated the chemical and physical measurements in this classic ferromagnetic semiconducting material.

We have futhermore, generalized our findings by extending our studies to other magnetic semiconductors, notably the Th_3P_4 type gadolinium sulfide and to the extended solid solution system Gd_xSe_{1-x}.

Europium oxide, EuO, is a ferromagnet which may be metallic, insulating or exhibit an insulator-metal transition. These differences, together with those observed in the infrared (IR) absorption spectrum, are most likely related to the stoichiometry of the crystals. In order to examine this supposition in detail, we have studied the relationship of the IR[1] and the conductivity to the growth temperature and starting composition. We have found that systematic changes in these parameters result in systematic changes in the conductivity, IR absorption and the stoichiometry of the crystals. Some aspects of the problem have been examined by Oliver, et al[2] in their work on the conductivity of EuO.

Although both transport and magnetic measurements have been reported on various rare earth Th_3P_4 type structures,[3] to the best of our knowledge only very few examples of systematic studies on either of these properties exist. Interest in these substances is twofold: First of all the $Re_{3-x}v_xX_4$ (X = S, Se, Te) ($0 \leq x \leq 1/3$) change continuously from metals to insulators with increasing vacancy (v) concentration, x, leading to a variety of

cooperative effects such as superconductivity and ferromagnetism;[3] secondly, as was first recognized by the authors of Ref. 4, the random distribution of vacancies at the Th sites leads to fluctuating repulsive potentials and tailing of the conduction band in which the electronic states are localized. The purpose of this study is to present magnetic and transport measurements on magnetic $Gd_{3-x}V_xS_4$ and to interpret them, in part, in terms of the concepts developed by Cutler and Mott[4] for paramagnetic $Ce_{3-x}V_xS_4$.

During a recent attempt to grow crystals in the Gd_3Se_4-Gd_2Se_3 system in the vicinity of the 3:4 composition, the primary crystallization phase was found to have a NaCl type structure with a deep blue metallic color, the remaining phase being a eutectic composition of NaCl and the Th_3P_4 type defect structure. The blue phase had a smaller lattice constant than that expected for GdSe.

There has been evidence for some time in the literature, of compositional variation in the trivalent monochalcogenides. Iandelli[5] noticed a color variation from yellow gold to red violet in the sulfides and selenides, which he attributed to incomplete or non-homogeneous reaction. These were polycrystalline materials which were reacted in quartz at temperatures up to 1450°C. M. Guittard[6] studied the range of homogeneity of all the rare earth monosulfides using lattice constant variations of polycrystalline material to explore the range of solid solubility. She found that the range of homogeneity increased with atomic number. Furthermore, she determined from density measurements that the solid solubility was on the metal-rich side with sulfur vacancies for all the rare earth sulfides except Lu, for which the homogeneity range extended to both sides of the stoichiometric composition. In all cases the lattice constant increased with increasing sulfur concentration.

The rare earth monochalcogenides are gold colored because the electron not used in bond formation is believed to be in a band formed by 5d and 6s wave functions giving rise to the metallic character. The $^8S_{7/2}$ ground state of Gd^{+++} provides an atomic moment of $7\mu_B$ and is, as a pure spin state insensitive to lower order crystalline field splittings. The Gd-Se system was chosen for a study of compositional variation in the monoselenides since the interpretation of magnetization data does not present the complication of having to consider orbital contributions to the magnetic moment.

2.0 THE EUROPIUM OXIDE SYSTEM

Crystals of EuO were synthesized by reacting Eu-metal and Eu_2O_3 at high temperatures, i.e. 1450-2100°C.[7] Since EuO at these temperatures loses Eu,[8] the crystals were grown in sealed tungsten crucibles from Eu rich starting mixtures which varied from 50-35 mol % oxygen. The resulting crystals, as we shall show, can be grouped into five classes according to their physical properties. The growth parameters as well as the physical properties of crystals in these five classes are summarized in Table I.

All crystals grown in the temperature range defined by Region I were found to have an IR absorption spectrum similar to that labelled I in Fig. 1. This spectrum is the same as that of Eu_3O_4, indicating that in these crystals Eu_3O_4 was present as a second phase. This supposition was confirmed by metallographic and x-ray analyses. The intensity of this absorption was weaker for crystals richer in Eu and was absent in crystals whose starting composition was less than 40 mole % oxygen. EuO crystals from Region I, therefore, lose some Eu and precipitate a second phase of Eu_3O_4 (Table I).

Crystals from Region II showed no Eu_3O_4 absorption, but did have sharp absorption lines near 3117 and 4848 cm^{-1} as shown on Fig. 1. These lines are characteristic[9] of Eu^{3+}, which would be expected in the EuO lattice if Eu vacancies were also present. The absorption intensity of these lines was, therefore, taken as a measure of the number of Eu vacancies and was observed to be weaker in samples grown from richer Eu solutions. Crystals from Region III had no Eu^{3+} absorption and, in fact, had only weak absorption (typically $0.5 < \alpha < 5$ cm^{-1}) between the strong lattice absorption below 600 cm^{-1} and the electronic absorption above 7500 cm^{-1}. These crystals, with minimal absorption over a wide range of frequency, are closest to 1:1 stoichiometry. Crystals grown with even more excess Eu show a new IR absorption spectrum

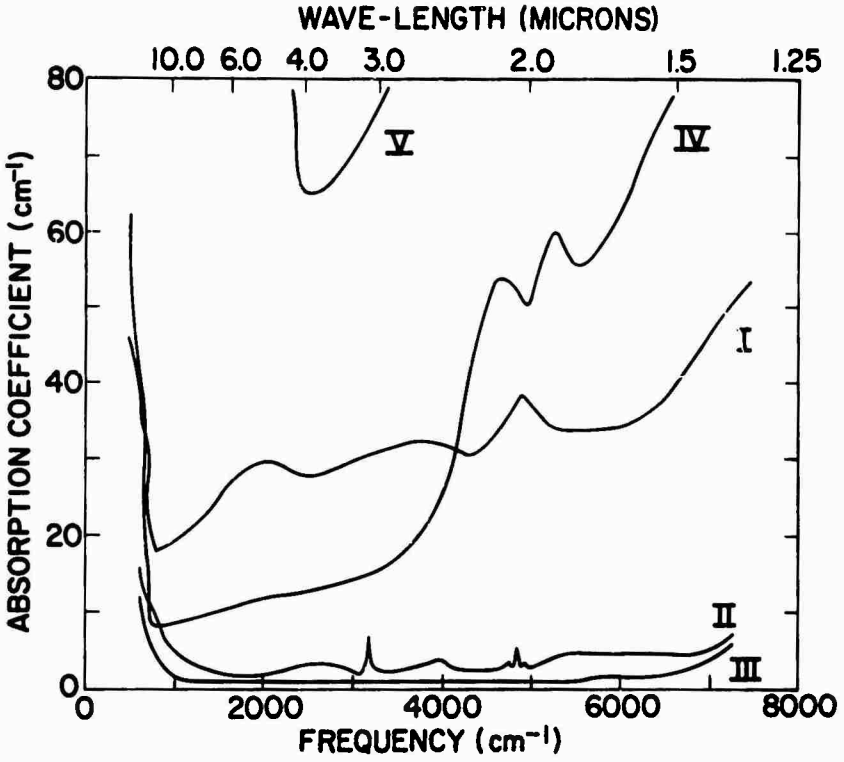

Figure 1 IR Absorption at Room Temperature for Different EuO Compositions

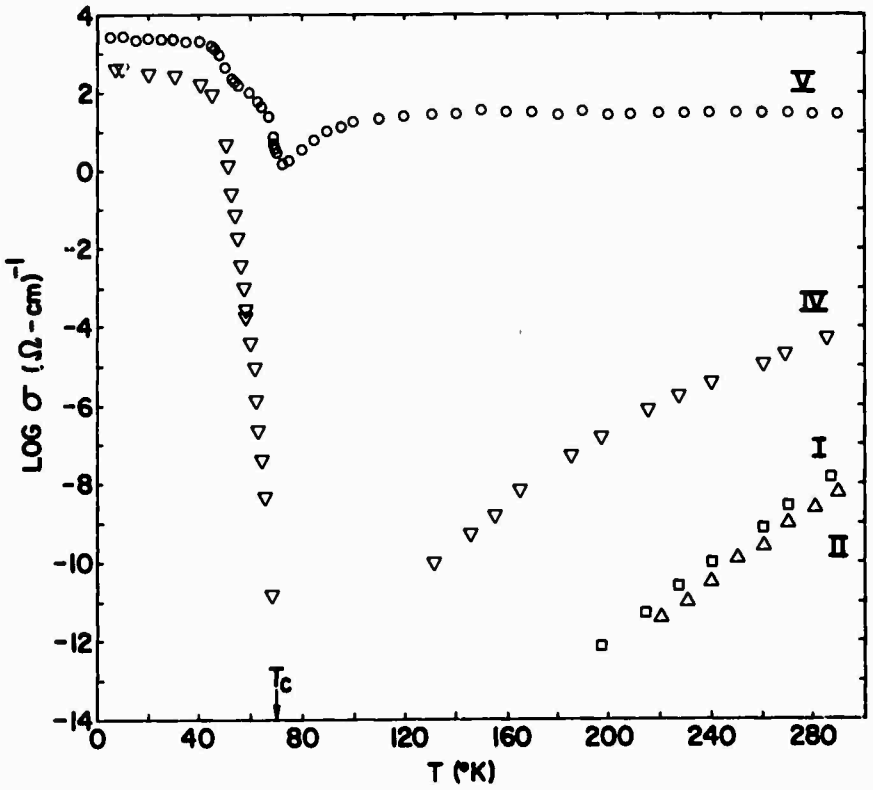

Figure 2 Conductivity vs Temperature for Different EuO Compositions

(curve IV, Fig. 1). This absorption increases with decreasing oxygen content in the starting mixture and finally the spectrum V is observed. It is natural to associate these spectra with the presence of oxygen deficiencies (probably vacancies) in the crystals. The low frequency portion of the Region V spectra show metallic absorption.

The electrical conductivity of crystals from Regions I and II are all very similar and typical results are shown in Fig. 2. All crystals from these regions are quite insulating, with thermal activation energies of 0.6 ± 0.1 eV and room temperature resistivities of 10^6 - 10^8 Ω cm. These results are consistent with the characterization of Regions I and II from IR and metallographic results. The conductivity of Region IV crystals is particularly dramatic, exhibiting an insulator-metal transition[2,10,11] below the Curie temperature (69.3°K) as shown by curve IV in Fig. 2. Near this temperature the conductivity may change by more than 13 orders of magnitude. From this work we expect these samples to have oxygen deficiencies of some sort. In fact, the existence of the insulator-metal transition has been theoretically related to the presence of oxygen vacancies.[2] Crystals from Region V are metallic at all temperatures (curve V, Fig. 2). Since oxygen vacancies are donors in EuO, they merge with the bottom of the conduction band at these large concentrations, giving metallic conduction.

From the results of these IR and conductivity measurements, together with a metallographic and x-ray study of quenched samples, we were able to construct the phase diagram shown in Fig. 3. First; there is appreciable compositional variation in the EuO phase, on both the oxygen-rich and Eu-rich side of the stoichiometric composition. We show the maximum width to be about 2-3%, in rough agreement with the composition at 1500°C reported in Ref. 13. Recognizing the difficulty in using conventional techniques to determine small compositional

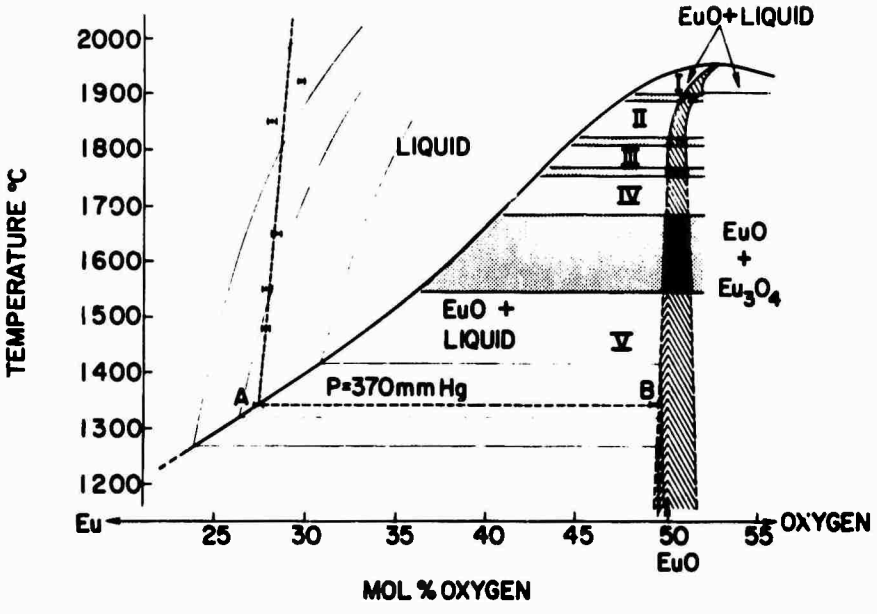

Figure 3 Partial Phase Diagram for the Eu-O System

ranges on this, we have used data from several sources to arrive at the 2-3% range. These data, from microstructure, chemical analyses, carrier concentration, and Mossbauer measurements were all consistent with this value. However, each of these measurements alone would probably not be sufficient for us to arrive at this value. Second; above ∿ 1825°C EuO is always oxygen-rich. This fact is due to a preferential loss of europium[8] which cannot be prevented by adding excess Eu-metal to the closed crucible. Third; it is possible to grow EuO crystals from a liquid phase at much lower temperatures (∿ 1450°C) than was previously thought possible.[7,14] Finally; from the phase diagram it is possible to select the proper composition and growth temperature so that EuO crystals can be grown with the desired stoichiometry.

In Fig. 3, the heavy dashed line shows the composition of the liquid and solid phases in equilibrium with pure europium vapor. There is a univariant point at 1355°C (point A) where three phases, liquid (A), solid (B) and vapor (P_{Eu} = 370 mm, the vapor pressure of Eu at this temperature) are in equilibrium. Further lowering of the temperature or the Eu-pressure will result in the liquid being converted to an oxygen deficient solid (B). This diagram was determined under conditions where all reactions were carried out in closed containers so that it was not possible to vary the pressure independently. It therefore represents a curved surface which cuts across the volume defining the P-T-X diagram for the europium oxygen system.

Because of the concentration gradients, a usual difficulty of melt grown "non-stoichiometric" crystals, it is difficult to specify a distinct boundary between adjacent regions (I, II, III, etc.) of the diagram. For example, the first part of the crystal to freeze may contain some Eu^{3+} (Region II) while it may be absent in the last part to freeze. For this reason, broad boundaries between the regions are shown in Fig. 3 - particularly between Regions IV and V.

3.0 THE FERROMAGNETIC SEMICONDUCTOR $Gd_{3-x}V_xS_4$

3.1 Experimental

Crystals were grown from previously synthesized compositions in sealed W crucibles by heating to the melting point and cooling slowly to room temperature. The resulting material does not show any easy direction for cleavage and magnetic measurements were performed on small samples of arbitrary shape. D.C. transport measurements, however, were made on crystals shaped as rectangular parallelopipeds.

Our present investigation of the $Gd_{3-x}V_xS_4$ system extends over a very limited range of compositions, $.318 \lesssim x \lesssim .326$. For these compositions ferromagnetic behavior is observed as shown in Fig. 4a and 4b. Figure 4b gives the 4.2°K magnetization data which shows a pronounced field dependent moment for both compositions. The projected zero field magnetic moment is 43 and 55 emu/gm respectively for I and II which represents only between 1/4 and 1/3 of the 190 emu/gm calculated for complete alignment of the Gd^{3+} moments.

For sample I the temperature-moment curves indicate that the Curie point, T_c, is $\sim$ 15°K. On sample II measurements in the range 5 to 50°K are lacking. A third sample from the same boule as II gave values $\theta \gtrsim 19$°K and $T_c \gtrsim 19$°K. Evidently, small variations in composition exist.

Figure 4b indicates that the paramagnetic susceptibility, χ, follows a Curie-Weiss law, $\chi = C/(T - \theta)$, where C is the Curie constant. From the linear dependence of $1/\chi$ on temperature we conclude that the material is not ferrimagnetic, which almost always results in a negative θ intercept rather than the observed positive values of 16.1 and 22.2°K. The molar Curie constants, C_M, derived from the slopes of Fig. 4b are 7.51 and 7.56 for samples I and II respectively. These values are $\sim$ 5% lower than $C_M = 7.87$ calculated for Gd^{3+}.

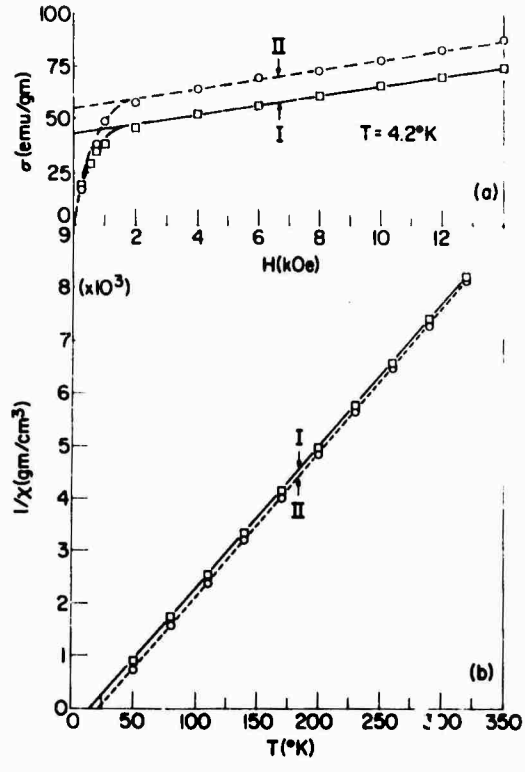

Figure 4a Magnetic Moment, σ, vs Applied Magnetic Field, H, at 4.2°K

Figure 4b Temperature Dependence of the Inverse Susceptibility, $1/\chi$, for Two Compositions, I and II

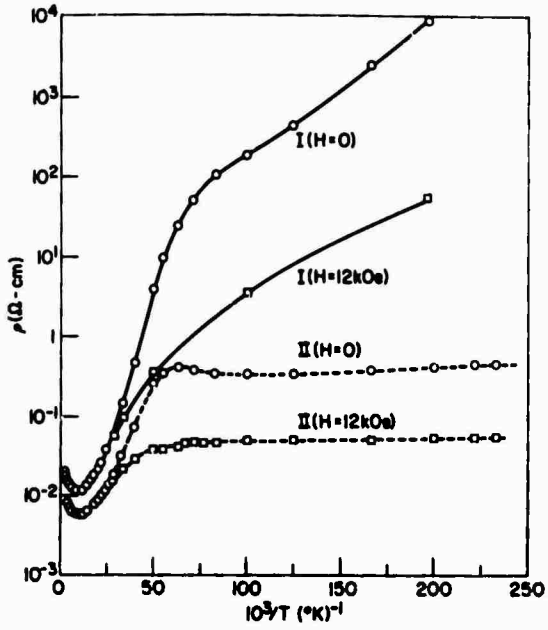

Figure 5 Resistivity, ρ, vs Reciprocal Temperature. The Paramagnetic Curie Temperatures are θ(I) = 16.1°K and θ(II) = 22.2°K.

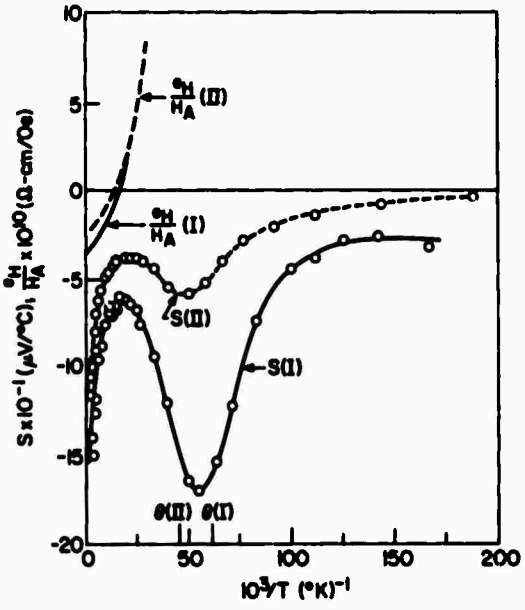

Figure 6 Hall Coefficient, e_H/H_a, and Seebeck Coefficient, S, vs Reciprocal Temperature

We speculate that the materials either form a canted structure[15] or that the results represent a superposition of several magnetic phases.

The results of the resistivity, ρ, with and without an applied field of 12 kOe as a function of temperature are exhibited in Fig. 5. The following features should be noted: (i) Both samples show a resistance minimum near 100°K; (ii) Between $\sim$ 100°K and $\sim \theta$, ρ is activated with an energy $E(I) \sim 1.7 \times 10^{-2}$ eV and $E(II) \sim 1.1 \times 10^{-2}$ eV. Below θ, ρ remains activated but with a significantly reduced activation energy; (iii) Application of a magnetic field reduces ρ and E below $\sim$ 40°K. It is clear that the negative magnetoresistance which is effected either by an applied magnetic field or by temperature (through the Weiss field), is related to the state of magnetic order.

Figure 6 depicts the results of thermoelectric power and Hall measurements. The Seebeck coefficient, S, becomes a minimum near 100°K, just as did ρ, rises to a maximum just above θ, and then decreases towards 0 as $T \to 0$. The sign of S is always <u>negative</u>. The Hall coefficient, e_H/H_A, is <u>negative</u> at room temperature but reverses sign near, but below, the temperature at which ρ is a minimum. For reasons discussed below, this sign reversal was unexpected and we have attempted to eliminate such spurious causes for anomalous Hall behavior as surface effects[16] and an unusually large Nernst-Ettinghausen effect. The former was tested by comparing the temperature dependent resistivities of samples with clean and lapped surfaces. No significant differences were observed. The latter was tested by comparing 210 hz and D.C. results[17] on sample II at 300°K and $\sim$ 56°K. Both the magnitude and sign of the Hall coefficient agreed. We were unable to make Hall measurements below $\sim$ 35°K because the onset of the large negative magnetoresistance masked the effect.

3.2 Discussion

If we restrict our discussion to the region above θ, $Gd_{3-x}v_xS_4$, exhibits resistivity characteristics (Fig. 5) very similar to those observed in $Ce_{3-x}v_xS_4$.[4] Cutler and Mott[4] analyze their data in terms of band conduction above the mobility edge at high temperatures and hopping conduction in localized states below this edge at low temperatures. The potential giving rise to this tail is attributed to the disordered vacancies in the Th_3P_4 structure. Besides the resistivity minimum in various samples of $Ce_{3-x}v_xS_4$, with x near 1/3, we note other similarities in transport phenomena. $|S|$ decreases linearly with decreasing T with a slope having non-zero intercept but in several cases starts to rise again in a manner similar to that shown in Fig. 6 below $\sim$ 100°K. The sign of S is always negative. Cutler and Mott[4] argue that hopping transport results in a linear dependence of S on T, i.e.

$$S = C_1 + C_2T \qquad 3.2.1$$

where C_1 and C_2 are constants, provided that the density of states at the Fermi energy, $N(E_F)$ and $\sigma(E_F) = 1/\rho(E_F)$ are appreciable. If this is not the case, these authors show that an increase in $|S|$ is expected, since transport will then be dominated by contribution of thermally excited electrons above the mobility edge. S as well as e_H/H_A are negative as expected, since the substitution of Ce atoms for vacancies adds electrons to the conduction band.

Since transport in the paramagnetic Ce system is satisfactorily explained in terms of localization of electron states, we shall adopt a similar point of view for its ferromagnetic counterpart $Gd_{3-x}v_xS_4$, with the additional hypothesis that at least part of the energy which localizes the electrons is magnetic in

origin. The idea of localization through exchange interactions, J_{c-f}, between conduction electrons and localized spins has been explored in detail with respect to the transport properties of NaCl-type Eu-chalcogenides.[18] We wish to note here only two properties of this magnetic binding energy, E_m: (i) E_m exists far above the magnetic ordering temperature because J_{c-f} is, in general, larger than J_{f-f}, the exchange primarily responsible for long range order, (ii) E_m approaches 0 with increasing magnetic order since J_{c-f} can no longer significantly alter the magnetic environment near the electron.

The gross features of the temperature dependence of the resistivity in samples I and II can then be explained as follows: (i) The approximately linear decrease in ρ between 300 and 100°K is dominated by lattice scattering of thermally excited band electrons; (ii) The activated process between $\sim$ 80 and $\sim$ 20°K is dominated by hopping in localized states (although thermally excited states may contribute); (iii) Near and below θ, the activation energy for transport becomes smaller due to the onset of magnetic order, as seen in Fig. 5 below $\sim$ 20°K. The qualitative behavior with an applied magnetic field follows, since, the magnetic field tends to decrease the binding energy for the electron and hence its activation energy.

The model is also consistent with the observed behavior of S if we accept the explanation for the low temperature rise in $|S|$ given by Cutler and Mott[4] i.e. that S is dominated by contributions from band states. The final reduction in $|S|$ below θ is then due to the reduction in magnetic binding energy which will increase the number of thermally excited carriers. Futhermore, fundamental considerations require that S approach 0 at $T \to 0$°K.

We believe that the sign reversal of the Hall effect is due to a contribution from the anomalous Hall constant, R_1, usually found in ferromagnetic materials. A plot of e_H/H versus χ for sample II (where the best data

is available) yields a straight line with slope $|R| \approx 7 \times 10^{-8}$ Ω-cm/G which is comparable in magnitude to values found in ferrites[19] where conduction is believed to occur in narrow d-bands. Further work is necessary to confirm this explanation.

4.0 THE Gd_xSe_{1-x} SYSTEM

4.1 Experimental

Since among other measurements, we elected to examine transport properties and reflectivity as a function of concentration, it became apparent that it would be useful to obtain single crystals. In order to study the homogeneity range, two large charges on either side of the stoichiometric composition were synthesized using the following procedure: All materials were handled in a He purged dry box. Metallic Gd sponge obtained from the Lunex Corp. having a nominal 99.9 concentration and 99.999 Se from the United Mineral and Chemical Corp. were reacted by the vapor transport of Se to the gadolinium side of an evacuated and sealed dual chamber quartz reaction tube. This reaction was carried out at a maximum temperature of 600°C because at higher temperatures there was evidence of quartz attack. Transport was considered complete when the characteristic color of Se vapor disappeared. The product of this reaction is quite inhomogeneous. The entire charge was transferred to a large tungsten crucible which was covered and sealed by electron beam welding. The crucible was then heated to 1600°C in a vacuum heated RF furnace. The two samples were powdered and chemical analysis gave the Gd rich composition as $GdSe_{.96}$ and the Se rich composition as $Gd_{.72}Se$. A series of samples developed from mixtures of these two compositions were used for crystal growth. Samples of approximately 6 grams were pressed into pellets which were sealed into 3/8 x 2 in. tungsten crucibles. Crystals were grown in an induction heated RF furnace using a 10^{-6} torr vacuum to protect the crucible from surface reaction. Temperature measurement and control were achieved with an NBS calibrated L&N automatic optical pyrometer, surface temperature having been calibrated with a black body

measurement obtained with the same geometry. Samples were heated to the melting point and cooled at about a degree per minute to 700°C at which point the power was turned off.

X-ray data were obtained with a Guinier focussing camera using Si as an internal standard. A least squares fit to the data gave a standard deviation of 0.001 Å.

Relative sample concentrations were obtained using an ARL EMX-SM electron microprobe with Gd metal as a standard. The error in concentration from sample to sample was estimated to be of the order of 0.5%. The composition scale was fixed with wet chemical analysis of three of the microprobe samples. Gd was determined by an EDTA titration and Se by a permanganometric titration. The error in the analysis was estimated to be of the order of 1%.

An AEI MS-7 double focussing solid state mass spectrometer was used for impurity analysis of the Gd metal and several single crystals of the selenide. Y and Ho were found in the 100-200 ppm range and Cu, Si, O, C and Na at the 100-300 ppm level. Synthesis and crystal growth of the selenide led to small increases in Na and Cu concentrations and considerable reduction in the C and O impurity levels. Since the small increase in Na and Cu concentrations (about 50 ppm) was not found to scale with Gd content, the effects of impurities on physical properties were considered to be negligible.

Magnetization data were obtained with a force balance in fields up to 20 Kilogauss in the temperature range 4.2°K to room temperature.

A Cary 14 R spectrometer, modified with a reflectivity jig for 10° incidence was used for measuring the shift in reflectance spectra with composition. Instrumental corrections were obtained with an evaporated gold film standard.

A standard 5 probe D.C. technique was used to measure the resistivity as a function of temperature as well as the Hall effect, wherever possible. Measurements were limited to signals greater than 10^{-7} volts.

4.2 Results

A striking result of the crystal growth experiments is the dramatic variation of sample color as a function of composition. The Gd rich samples were a bright yellow gold color and as the Gd concentration decreased the color changed progressively to bronze, copper, red gold, purple and at the lowest Gd concentration, a deep metallic blue. Since there was a small temperature gradient along the crucible during crystal growth, a concentration gradient developed as the sample crystallized. Each single crystal ingot, therefore, graphically represented the crystallization process of the system. The initial crystallization was found to have the highest Gd concentration or most gold-like color and the final crystallization the lowest Gd concentration or most blue-like color, reflecting the range of solidus concentrations for a particular melt composition. Crystals of uniform color were cleaved from an ingot for analysis and it was found that by carefully matching the color of crystals from different areas it was possible to reproduce all physical measurements within the error of each determination. The gadolinium rich compositions were found to melt at approximately 2350°C. Melting temperatures decreased smoothly to about 1750°C for the blue, selenium rich phase.

Figure 7 is a plot of lattice constant as a function of concentration. The overall decrease of lattice constant with increasing Se concentration is unexpected and contrary to Guittard's[6] results for LuS. It is possible that density determinations will shed some light on the nature of the defect

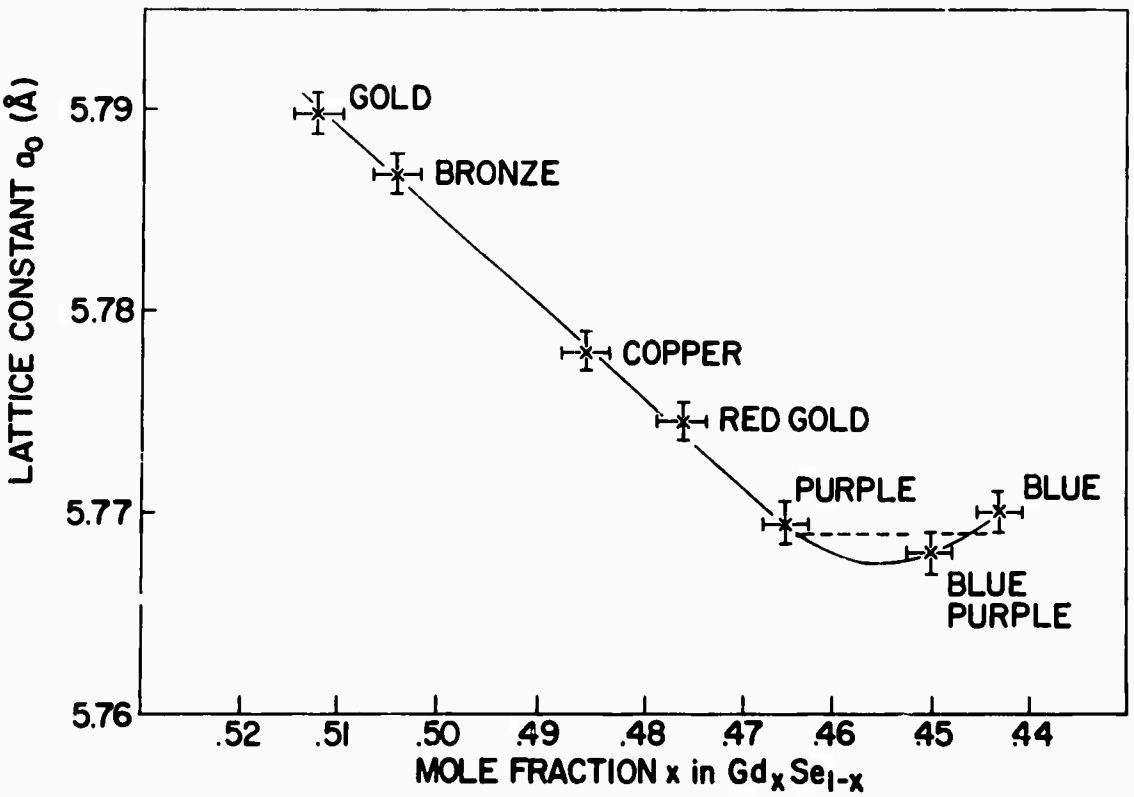

Figure 7 Lattice Constant a_o as a Function of Composition x in Gd_xSe_{1-x}

structure and provide an explanation for the lattice contraction. A straight line has been drawn through the stoichiometric composition. It is reasonable, however, to expect differences in slope on either side of this concentration. Although the data illustrates the general trend shown by the straight line, additional measurements are necessary to show any detailed changes in slope.

In the composition range x = 0.443 to 0.463 the lattice constant goes through a minimum as shown by the solid line. The lattice constant for the blue phase, (x = 0.443), is 5.770 Å, which is identical with the value obtained from the NaCl pattern of the two phase region. This composition therefore, represents the limiting concentration of the Se rich field.

It is also possible to draw a horizontal line (dashed line) which just touches the error bars for the three data points used to define the minimum. Such a line of constant a_0 would indicate that this is a two phase region. This would place the solubility limit in the Se rich field at $x \sim 0.465$. However, neither x-ray nor metallographic analyses showed any evidence of a second phase.

The results of the resistivity measurements can be summarized as follows: (i) The bronze and gold colored samples, which have comparably low resistivities, ρ, exhibit a temperature dependence in ρ normal for magnetically ordered metals (lower curves in Fig. 8). The resistivity is linear in the paramagnetic region with a knee near T_N and drops precipitously as the temperature decreases towards 0°K. This is readily analyzed with three contributions to the resistivity

$$\rho = \rho_L + \rho_i + \rho_m, \qquad 4.2.1$$

where ρ_L = lattice, ρ_i = impurity and ρ_m = magnetic contributions to the resistivity. For these two samples ρ_m is constant above T_N (only spin disorder

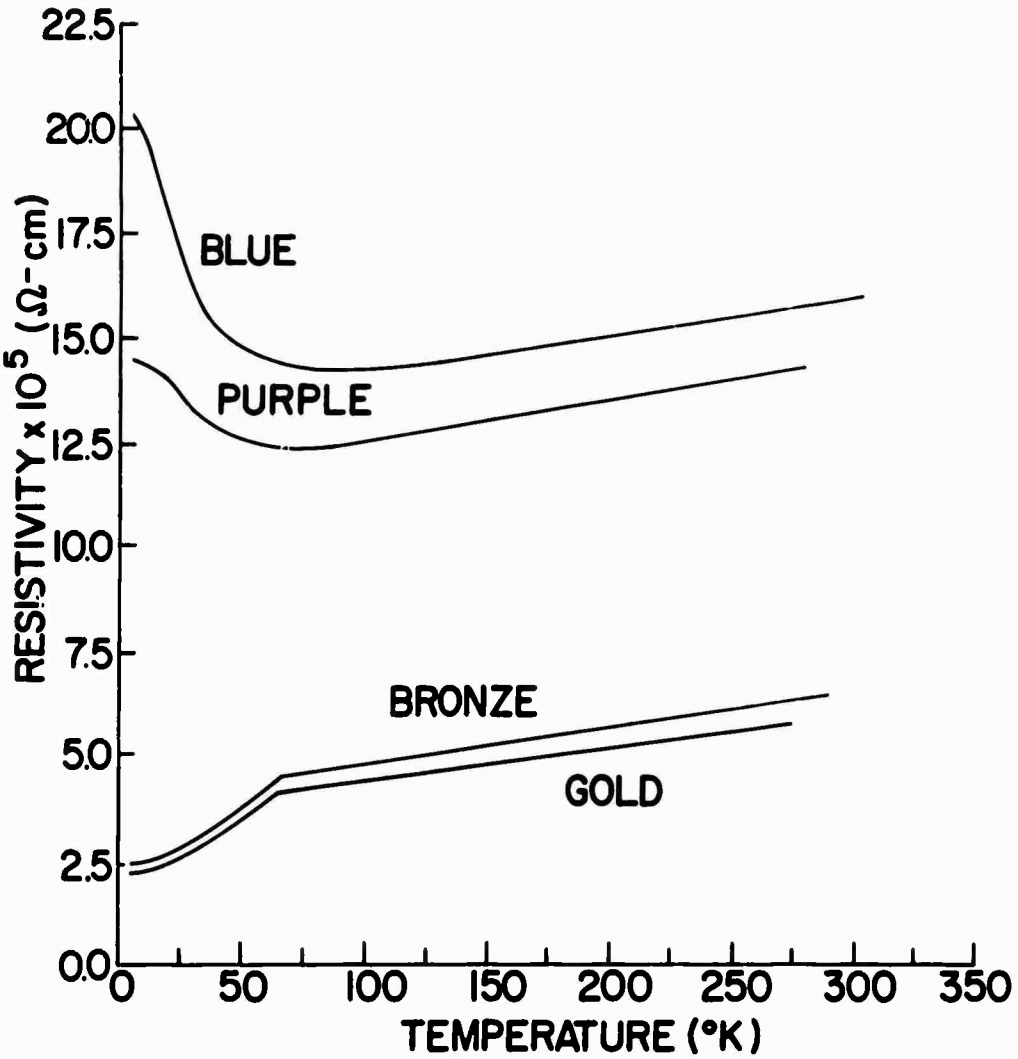

Figure 8 Resistivity, ρ, as a Funciton of Temperature (°K) for Four Compositions, x, in the Gd_xSe_{1-x} System

scattering) which accounts for the observed curve. (ii) The resistivity as a function of temperature for both the blue and purple samples are plotted in the upper part of Fig. 8. The room temperature resistivity is higher (because the free electron concentration is lower) and the linear decrease in ρ with decreasing temperature reaches a minimum near 75°K, thereafter increasing to a constant value at low temperatures. Again we might analyze the data with equation (4.2.1) with the assumption that ρ_m includes a critical scattering term. On the other hand T_N, from magnetic data has not changed appreciably and it is unlikely that the resistivity will remain constant below T_N.

The Hall effect was measured at room temperature for the purple sample ($Gd_{.465}Se_{.535}$) and the carrier concentration derived by assuming a simple band was $n = 1.4 \times 10^{22}$ cm^{-3}. It is possible to check the consistency of this number with other independent measurements as follows: If we assume that each Gd contributes one electron to the conduction band, simple valence arguments lead to the expression

$$N_o [3x - 2(1 - x)] x2 = n \qquad 4.2.2$$

where N_o = carrier concentration for the stoichiometric composition ($x = 0.5$) where x = composition. Solving for N_o, using the experimental values $x = 0.465$ and $n = 1.4 \times 10^{22}$ cm^{-3}, one obtains $N_o = 2.2 \times 10^{22}$ cm^{-3}. On the other hand we can also calculate N_o using the lattice parameter for stoichiometric material as $N_o = 4/a_o^3 = 4/(5.78 \times 10^{-8})^3 = 2.1 \times 10^{22}$ cm^{-3}. The agreement is very satisfying and lends evidence to our model of a simple rigid band in which the number of free carriers is determined by the stoichiometry.

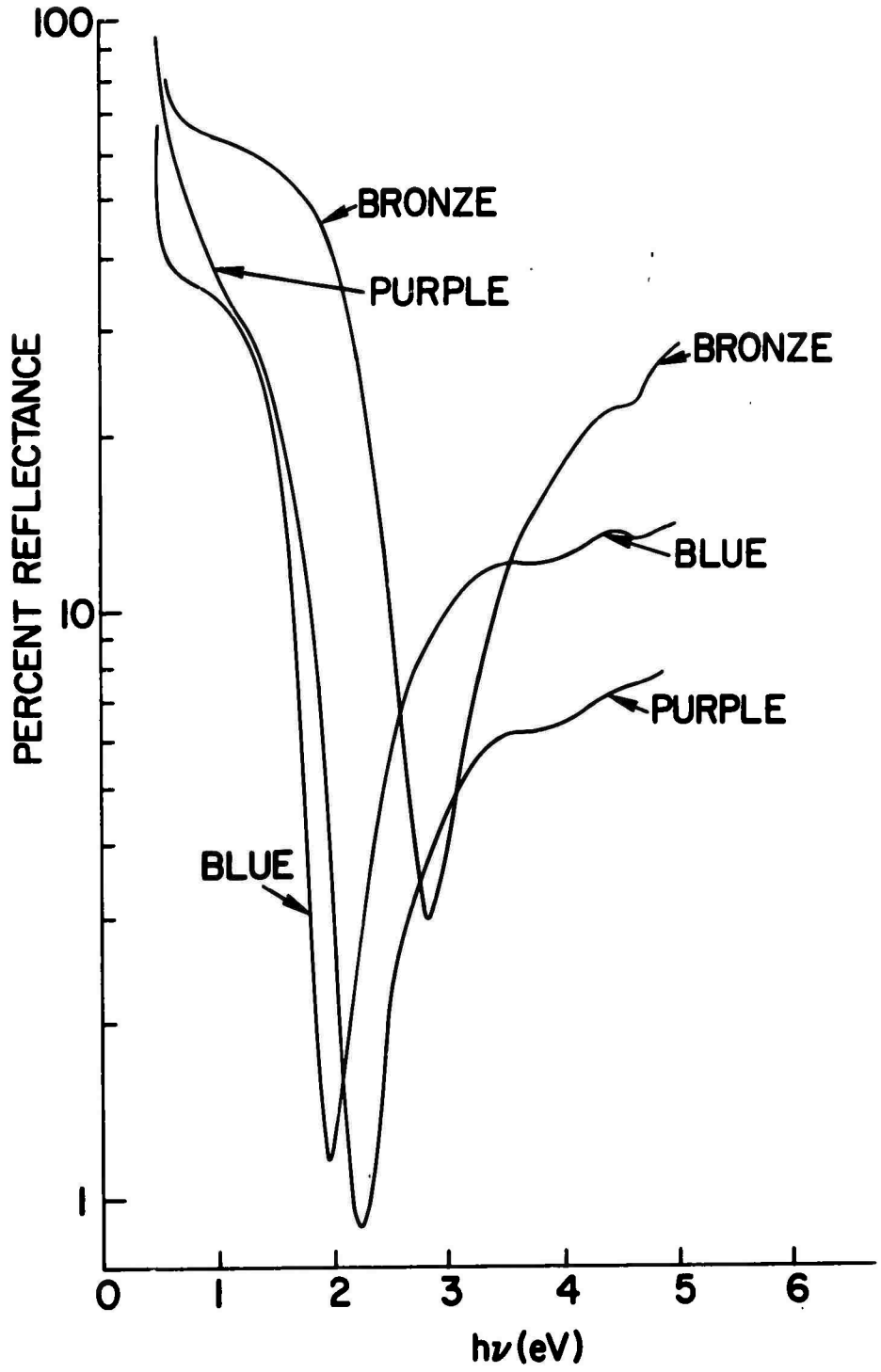

Figure 9 Percent Reflectance R as a Function of Energy hν

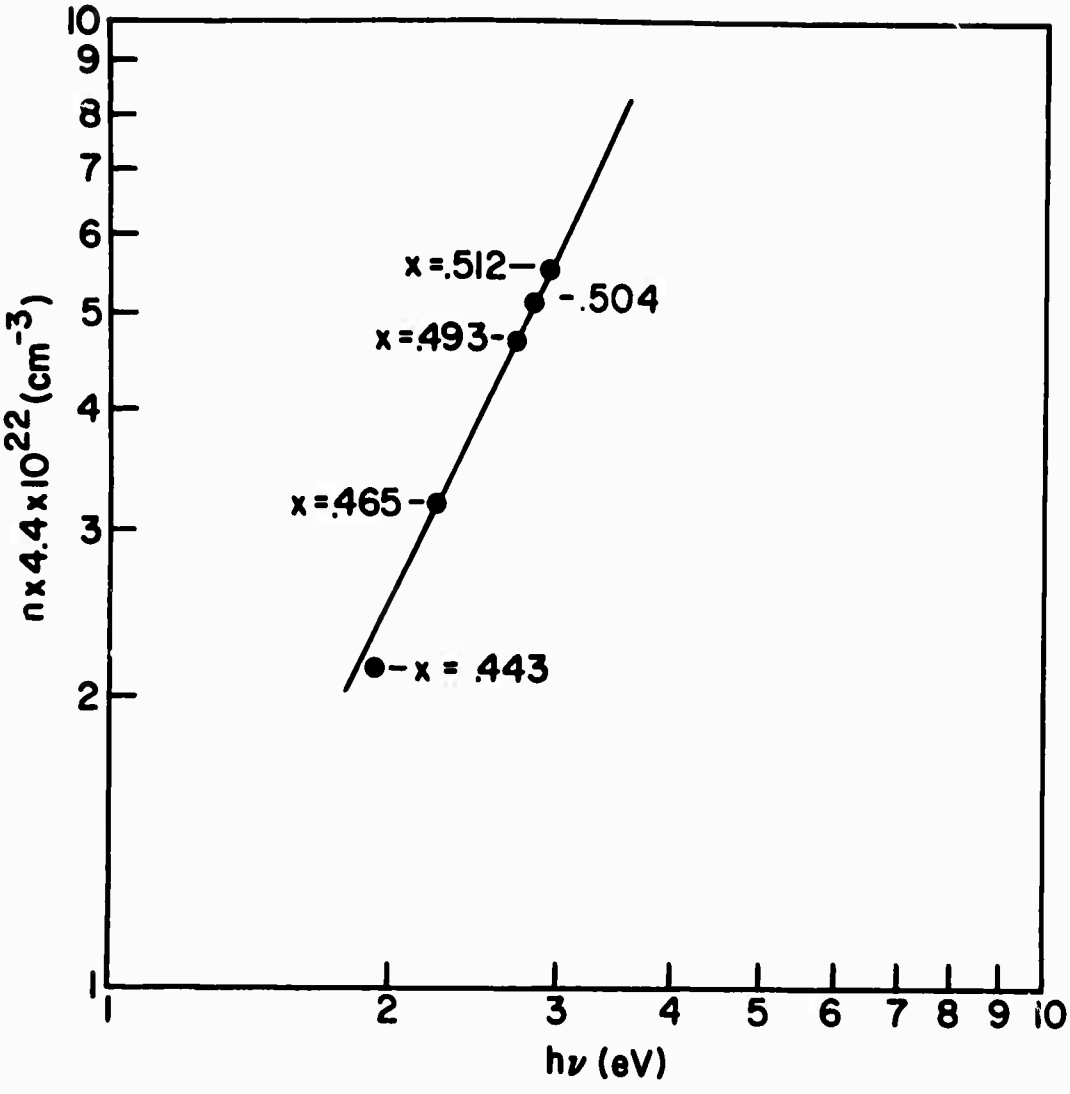

Figure 10 Carrier Concentration, n, Derived from Experimental Composition, x, as a Function of hν for Which the Reflectivity is a Minimum. The Data is Plotted on a Log-Log Scale to Demonstrate that $n \propto (h\nu)^2$ in the Gd_xSe_{1-x} System.

It is also tempting to attribute the dramatic changes in color simply to changes in carrier concentration. Figure 9 shows reflectivity data for three representative samples. For the case that the reflectivity minimum, R_{min}, is $\leq$ 5%, the dispersion relation for free carriers yields the following expression:

$$m_s \propto \frac{n \lambda_{min}^2}{\varepsilon_\infty - 1} \qquad 4.2.3$$

where m_s is the effective mass ε_∞ is the high frequency dielectric constant, n is the number of free carriers per unit volume and λ_{min} is the wavelength at which R_{min} occurs. Since $\nu \propto \frac{1}{\lambda}$, (4.2.3) can be rewritten as $(h\nu)^2_{min} \propto n$, and, assuming that m_s and ε_∞ do not vary substantially throughout the series, a plot of log n vs $h\nu$ should yield a straight line with a slope equal to 2. We have assumed here that the reflectivity is dominated by free carriers and that interband transitions, etc. perturb the spectra only slightly. Figure 10 exhibits the results of such a plot. It is apparent that the curve is consistent with our model with the exception of the lowest point.

All compositions in the solid solution system order antiferromagnetically. A rough measure of Néel temperatures indicates that they vary from $\sim$ 20°K for x = 0.443 to $\sim$ 60°K for x = 0.512. A plot of paramagnetic θ values as a function of composition (Fig. 11) is essentially linear with composition except for x = 0.443. Comparing these with the resistivity results we see that the negative exchange interaction increases strongly with electron concentration.

As we have shown the relationship between observed experimental parameters and composition is surprisingly direct, and in the case of resistivity and reflectivity is well explained by the simplest of all models, a single rigid band. It should of course be noted that in all cases the lowest Gd composition

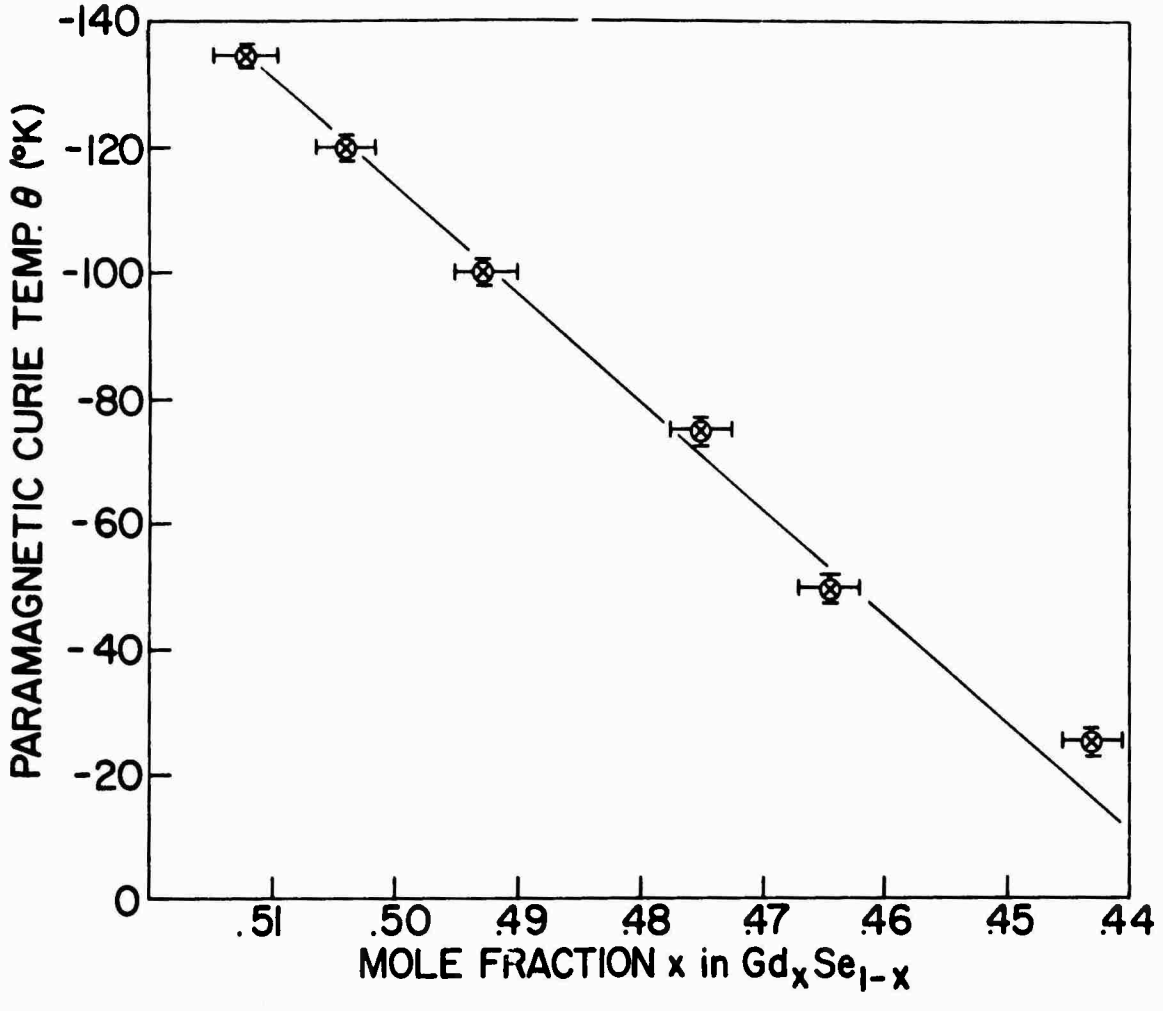

Figure 11 Paramagnetic Curie Temperature, θ, as a Function of Composition x, for Gd_xSe_{1-x}

appears to be anomolous, but the explanation probably lies in the breakdown of the free electron approach at lowest Gd concentrations. The possibility of two phases can be ruled out from the lattice constant argument given earlier as well as on the basis of a more detailed examination of the susceptibility data. The limiting concentration of the Gd - Th_3P_4 solid solution system forming the boundary of the two phase region is strongly ferromagnetic with θ positive and equal to 88°K.[20] Measurements on the eutectic phase also gave a positive θ. Any small amount of this ferromagnetic material in the composition $x = 0.443$ would show a deviation from the linear plot in Fig. 11 towards a more positive θ, which is contrary to experimental results.

References

1. J. B. Torrance provided the infrared data - this work was performed under ONR Contract No. N00014-70-C-0272.
2. M. R. Oliver, Ph.D. thesis, Dept. of Electrical Eng., M.I.T., June 1970 (unpublished).

   M. R. Oliver, J. A. Kafalas, J. O. Dimmock and T. B. Reed, Phys. Rev. Letters, 24, 1064 (1970).

   M. R. Oliver, J. O. Dimmock, A. L. McWhorter and T. B. Reed, Phys. Rev. B (to be published).
3. Landolt-Börnstein Tables, K. -H. Hellwege and A. M. Hellwege eds., 4a, pp. 41-109, Springer-New York (1970).
4. M. Cutler, J. F. Leavy and R. I. Fitzpatrick, Phys. Rev., 133, A1143 (1964); M. Cutler and J. F. Leavy, Phys. Rev., 133, A1153 (1964); M. Cutler and N. F. Mott, Phys. Rev., 181, 1336 (1969).
5. A. Iandelli, "Rare Earth Research" Ed. E. V. Kleeber, MacMillan, 1961, New York, Vol. 1, p. 135.
6. Mlle M. Guittard, Compt. Rend., 261, 2109 (1965).
7. M. W. Shafer, J. Appl. Phys., 36, 1145 (1965).
8. J. M. Haschke and H. A. Eick, J. Phys. Chem., 73, 374 (1969).
9. G. H. Dieke, "Spectra and Energy Levels of Rare Earth Ions in Crystals", Interscience, New York (1968).
10. G. Petrich, S. von Molnar and T. Penney, Phys. Rev. Letters, 26, 885 (1971).
11. T. Penney, M. W. Shafer and J. B. Torrance (to be published).
12. S. von Molnar and T. Kasuya, Proc. 10th Int. Conf. on Phys. Semiconductors, S. P. Keller, J. C. Hensel, F. Stern Eds. Conf. 700, 801, U. S. AEC Div. of Tech. Inf., Oak Ridge, Tenn., 1970, p. 233.

13. R. G. Bedford and E. Catalano, J. Solid State Chem., 3, 112 (1971).

14. T. B. Reed and R. E. Fahey, J. Crystal Growth, 10, 211 (1971).

15. P. G. de Gennes, Phys. Rev., 118, 141 (1960).

16. E. H. Putley, "The Hall Effect and Related Phenomena", Butterworth, London (1960).

17. Olof Lindberg, Proc. I.R.E., 40, 1414 (1952).

18. S. von Molnar and T. Kasuya, Proc. 10th Int. Conf. on Phys. of Semiconductors, S. P. Keller, J. C. Hensel, F. Stern, eds. Conf. 700, 801, U. S. AEC Div. of Tech. Inf., Oak Ridge, Tenn., 1970, p. 233.

19. J. M. Lavine, Phys. Rev., 123, 1273 (1961).

20. F. Holtzberg, T. R. McGuire, S. Methfessel and J. C. Suits, J. Appl. Phys., 35, 1033 (1964).